Molecular dynamics simulations of the transformation of carbon peapods into double-walled carbon nanotubes

I. Suarez-Martinez**, P.J. Higginbottom and N.A. Marks

Nanochemistry Research Institute, Curtin University of Technology, GPO Box U1987, Perth WA 6845, Australia

Abstract

The transformation of carbon peapods (encapsulated fullerenes in nanotubes) into double-walled nanotubes is studied using molecular dynamics simulation. The simulations reproduce the two main trends known experimentally: the production of low-defect nanotubes and the templating effect of the outer tube. The process involves a low-temperature polymerization of the fullerenes followed by higher temperature self-assembly into a tube. Modelling of this second stage is made possible by the use of the environment dependent interaction potential, a large number of atoms and long-time annealing. Analysis shows that the outer tube acts as a container for the self-assembly process, analogous to previous simulations and experiments in which free surfaces, either external or internal, template the formation of highly ordered sp^2 phases.

**Corresponding author. Fax: +61 8 9266 4699. E-mail address: I.Suarez-Martinez@curtin.edu.au (Irene Suarez-Martinez)

1. Introduction

Carbon nanotubes offer an internal volume that can be filled by many different molecules. When the enclosed molecules are fullerenes, the structure is known as a peapod. Peapods were first observed in low quantities in pulsed laser ablation experiments [1] and are now routinely generated in a multi-step process involving end-cap oxidation of single-walled carbon nanotubes (SWCNTs) followed by sublimation of fullerene powder [2,3,4]. Peapods have been studied for their unusual electronic [5,6] and optical [7] properties and have also found application as a precursor of double-walled carbon nanotubes (DWCNTs) [8]. Under electron irradiation [9,10] or thermal treatment under pressure [8], it has been seen experimentally that the fullerene molecules fuse and rearrange to form an inner tube. This "peapod route" provides a large scale synthesis method for producing DWCNT's in the absence of a catalyst and with high yields.

The encapsulation process is easily understood on thermodynamic grounds, being driven by van der Waals attractions which are maximized when the fullerenes are inside the nanotube and regularly spaced [11]. On the other hand, the process by which fullerenes fuse and transform into a nanotube is much less well understood. Motivated by calculations of nanotube-fullerene fusion [12], a fullerene fusion pathway based on [2+2] cyclo-addition and sequential Stone-Wales rotations was proposed by Han et al [13]. Despite its intuitive appeal, this process results in a tubular structure with the same radius as the initial fullerenes, in conflict with X-ray diffraction measurements [14] which show that the inner diameter is determined by the outer tube, the difference being twice the interlayer distance in turbostratic graphite (i.e. 0.36 nm). Another drawback of this model is that only Stone-Wales-

like rotations are considered, a restriction which may be unwarranted given that the peapod route involves temperatures over 1400 K [8].

Molecular dynamics (MD) provides an unbiased methodology for exploring fusion and transformation of peapods and is therefore an attractive alternative to static-based methods. Several MD calculations have been performed to date, using empirical potentials (Tersoff [10] and ReaxFF [15]) and tight-binding [10] methods. The longest simulations, following 300 ps of motion, were performed using the Tersoff potential [10]. Fusion of fullerenes was observed, but a DWCNT was not produced, and even at 3600 K the inner tube was highly corrugated. More accurate calculations using ReaxFF observed some covalent bonding between fullerenes, but were restricted for computational reasons to just 16 ps of simulation time [15]. Further ReaxFF calculations including Ni atoms showed additional cross-linking (due to the catalytic effect of Ni) but the final structure remained highly defective [15]. A similar approach was employed in tight-binding MD simulations, where a high vacancy concentration (2 per fullerene) was applied to accelerate the dynamics [10].

In this work we present MD simulations of DWCNT formation from peapods using the Environment Dependent Interaction Potential. Our simulations are distinguished from previous studies by the long simulation times (one nanosecond), the large number of atoms considered, and the absence of artificial acceleration techniques such as defects or catalysts. We observe both stages of DWCNT formation from peapods, an initial polymerisation step in which fullerenes are linked, and a much slower process in which the atoms rearrange to form a tube. In agreement with experiment,

we find that the diameter of the inner tube is determined by the outer tube. This demonstrates that the fusion of fullerenes into a nanotube is inherently a self-assembly process [16] templated by the outer tube.

2. Method

Molecular Dynamics simulations were performed using the Environment-Dependent Interaction Potential (EDIP) for carbon [17,18]. Originally developed to study amorphous systems with a high sp^3 content, EDIP has more recently been applied to self-assembly in a variety of sp^2-bonded systems including carbon onions [19], nanotubes and glassy-carbon-like foams [16]. Based on an earlier EDIP potential for silicon [20], carbon EDIP employs an atom-centred bond-order term and a generalised coordination term which captures dihedral rotation and π-π repulsion. In the context of the present study, the atomic bond-order predicates against a correct description of [2+2] cyclo-addition known to occur in fullerene fusion; we will return to this point later. For computational reasons (EDIP was developed with thin-film deposition in mind) the potential falls to zero beyond 3.2 Å and accordingly adjacent graphene sheets do not experience Van der Waals attraction. Perhaps surprisingly, this does not affect the simulations in this work as discussed below. Closer interactions, however, are described appropriately, with EDIP and density-functional-theory (DFT) in good qualitative agreement for the energy barrier between rhombohedral graphite and diamond. This parametrization with respect to DFT gives EDIP a significant advantage over the Tersoff and Brenner potentials where the use of arbitrary cutoff functions leads to qualitatively incorrect barriers for bond-making and bond-breaking processes [21,22]. Another advantage of EDIP is speed of the calculation, offering a significant performance improvement relative to ReaxFF and tight-binding MD,

thereby enabling the study of large system sizes and long simulation times reported in this work.

Two peapod systems were studied, each containing 21 C_{60} molecules. Previous MD studies have considered much smaller systems (4 fullerenes in the case of the tight-binding studies [10], and 5 and 10 fullerenes for the ReaxFF [15] and Tersoff [10] potential simulations, respectively). Periodic boundary conditions were applied along the tube axis, and in both systems the box length was 224.82 Å. The systems different only in the chirality and radius of the encapsulating tube, the smaller system being a (13,7) CNT of radius 13.76 Å, the larger being a (12,12) CNT of radius 16.27 Å. Both nanotubes were relaxed within the EDIP formalism, and the primitive cell was repeated 9 and 91 times for the small and large radius system, respectively. The C_{60} molecules were also relaxed prior to encapsulation, with EDIP overestimating the diameter by 4.1% due to the fixed aromaticity associated with the atomic bond-order. The C_{60} molecules were homogenously distributed along the tube axis, corresponding to a separation distance between fullerene walls of 3.25 Å. Since this is greater than the EDIP cutoff, initially the fullerenes do not interact. A similar situation applies for the fullerene-nanotube interaction, for which the separation distances are 3.21 and 4.56 Å for the small and large radius systems, respectively. The total number of atoms in the system was 4968 for the (13,7) peapod, and 5628 for the (12,12) peapod. The equations of motion were integrated within an NVE using the Verlet method with a timestep of 0.35 fs. Velocity rescaling thermostats were applied to constrain the average temperature fluctuation within the range $\Delta T/T < 1.5/\sqrt{N}$, where N is the number of atoms in the simulation. This inequality restricts the temperature fluctuations within the limits appropriate for an infinite system.

Both peapod systems were annealed for one nanosecond at temperatures spanning 1500 to 4000 K. The temperature profile early in the 3000 K anneal is shown in Fig. 1. Five stages are present, the first two being associated with equilibration to the desired temperature. In stage (1) the system is equilibrated at 300 K prior to annealing, while in stage (2) the temperature is increased to the annealing temperature. In stage (3) the system is maintained at the prescribed anneal temperature and allowed to evolve for 5 ps. In stage (4) a branch simulation is initiated and the system is cooled rapidly to 300 K. Thermal averages for analysis are collected at 300 K in stage (5). These final three stages are repeated 200 times, giving a total annealing time of 1 ns. Note that each successive annealing cycle continues on from where the previous stage (3) anneal finished.

3. Results and discussion

Annealing simulations for the (13,7) and (12,12) systems were performed for six different temperatures between 1500 and 4000 K. Snapshots of the initial configuration and the final structures after 1 ns of annealing are shown in Figures 2 and 3. In both cases, polymerization of encapsulated fullerenes is observed at low temperatures, while at higher temperature transformation into a DWCNT is observed. In the case of the smaller (13,7) peapod, the DWCNT portion is 2/3 the length of the system, in agreement with experimental observations [8]. This “filling-factor” can be understood on the assumption of conservation of surface area: calculations presuming that fullerenes convert into a nanotube of identical radius show that with increasing number of fullerenes the nanotube length rapidly converges to a value 1/3 shorter than

the original array. Previous atomistic simulations failed to see this filling-factor effect, as the system size and potentials used precluded against separation of the inner tube into discrete regions of nanotube and free space. For the larger (12,12) peapod, the DWCNT portion is shorter, indicating that the radius of the inner tube is greater than that of the fullerenes. Slight differences between the (13,7) and (12,12) systems are also seen at the highest temperature considered, 4000 K. The smaller system shows kinks in the outer tube due to mass transport. The higher strain and high temperature leads to atoms being lost from the outer wall and also transferred between walls. In the larger radius system these processes do not occur at this temperature.

It should be noted that the annealing temperatures in the simulation are necessarily larger than their experimental equivalents due to the short timescale of molecular dynamics. By using annealing temperatures higher than those used in experiments, we are able to observe thermally activated processes which would otherwise not occur. The main proviso is that the annealing temperature must be below the melting point, a requirement that is met here. It is also relevant to note the similarity between transformation of fullerenes into a nanotube and previous EDIP simulations of sp^2 ordering and self-assembly [16,19]. The general trends with increasing temperature are almost identical, highlighting universal behaviour in annealed carbon systems.

To track the transformation of peapods into a DWCNT we computed the fraction of sp^2 atoms within the 1260 atoms making up the initial 21 fullerenes. Atoms were considered sp^2 bonded if three neighbours were found within a 1.85 Å cutoff. Figure 4 shows this sp^2 fraction as a function of temperature and time for the (13,7) system;

the larger system shows similar behaviour. At low temperatures the sp^2 fraction slowly decreases and eventually plateaus, reflecting the small number of sp^3 atoms associated with polymerization of the fullerenes into an extended chain. At higher temperatures, a more aggressive coalescence occurs, reducing the sp^2 fraction to about 80% in a rapid process. This is followed by a more gradual recovery of sp^2 bonding in which the merged fullerene units transform into the inner wall of the DWCNT. This second stage has not previously been observed in MD simulations of peapod coalescence. As can been seen in Figure 4, the recovery and transformation is rather gradual, requiring at least 600 ps, while previous MD calculations typically considered less than 100 ps [10,15]. Only Tersoff-potential simulations were run for longer (300 ps), but these calculations are limited by incorrect kinetics associated with the nearest-neighbour switching function. This deficiency is particularly apparent in simulations of amorphous carbon where the Tersoff potential predicts qualitatively incorrect structures [23,24,25].

Ring analysis offers a complementary description of the transformation process, showing how the topology changes over time. Figure 5 shows ring statistics for the 1260 atoms making up the initial 21 fullerenes, with the values reported normalised per fullerene. Figure 5(a) distinguishes clearly between polymerization at low temperature, and DWCNT formation at high temperature. For low temperatures, the difference between the number pentagons and heptagons is constant and equal to twelve, following the Euler relation for polygons on a sphere [26]. Transformation into a tube-like structure occurs at high temperatures with the residual pentagons associated with the end-caps. While the pentagon-heptagon difference is ideal for illustrating the fullerene/DWCNT transformation, it does not distinguish between

perfect and corrugated tubes. In order to assess the degree of order in the tubes, we computed the number of hexagons [Fig. 5(b)]. For the lowest temperatures considered, the number of hexagons increases slightly over time due to the increased connectivity associated with polymerization. We do not observe [2+2] cyclo-addition; instead fullerenes polymerize by forming three new bonds. This is not surprising due to the fixed aromaticity implicit in the EDIP formalism. We are not concerned with this polymerization process as C_{60}-dimerization has already been described with accurate quantum methods such as DFT [27,28]. Instead, our purpose is to allow fullerene units to fuse, and then study the conformational changes which occur when high-temperature annealing allows this system to explore its configuration space. It is in this second regime that EDIP is especially powerful, allowing study of the self-assembly process in a variety of ways that have previously not been possible.

Returning to the discussion of Fig. 5(b), the more significant trend is the time-variation at higher temperature, where the number of hexagons first decreases and then subsequently recovers. This behaviour is very similar to that observed for the sp^2 fraction in Figure 4; the polymerization is associated with a reduction of hexagons, while the recovery of the number of hexagons reflects subsequent self-assembly into an almost-perfect inner tube. This contrasts with all of the previous simulations where corrugated tubes were observed, and the Tersoff simulations [10] in particular where the inner wall was primarily a Haekelite structure [29].

We now consider the effect of varying the radius of the enclosing tube. As noted earlier, experiments [8,14] show that the interwall spacing is independent of the outer

tube, and is always close to the interlayer spacing in graphite. Correspondingly, the inner radius is a function of the outer radius, implying that the transformation mechanism is more complex than simple fullerene fusion, since this would preserve the radius of the inner tube. An outer-radius effect has already been shown in Figure 2 where it is apparent that for the larger system the inner tube is shorter. This reduction in length reflects an increase in the diameter of the inner tube as illustrated by the cross-sectional slice in Figure 6. In the (12,12) system the fullerenes transform into a tube 2 Å larger in diameter than for the (13,7) system.

We further quantify the radius effect in Figure 7 by computing radial distribution profiles with respect to the tube axis. To minimize the effect of undulations throughout the length of the system, the tube axis is determined via the centre of mass of thin slices. Three profiles are shown: (i) the initial peapod structure in which all atoms are in ideal locations, (ii) the final structure after annealing at 1500 K where the structure of the fullerenes has disappeared, and (iii) the final DWCNT structure corresponding to the annealing conditions in Figure 6. Considering first the (13,7) system, we see that for all three profiles the peak near 7 Å, corresponding to the outer wall, is unchanged. The peaks at shorter distances evolve with temperature, initially exhibiting a series of sharp peaks associated with the fullerenes, tending towards a Gaussian-like peak at 3500 K associated with DWCNT formation. The inner tube of the DWCNT has the same radius as C_{60} since the (13,7) tube exactly encapsulates the C_{60} molecules, neither compressing them nor providing room for off-axis motion. This geometry is the most common in simulations performed to-date. Considering now the (12,12) system, we see again that the outer tube remains unchanged upon annealing. However, the peaks at shorter distance evolve not only in shape but also to

larger radius as indicated by the white arrow. This demonstrates theoretically for the first time how the outer tube dictates the inner tube radius. For our (12,12) system we observe $D_{inner}=D_{outer}-2\times3.5$ Å, very similar to what has been observed experimentally [14]. Based on the interwall spacing of 3.5 Å it is tempting to infer that this expansion is driven by van der Waals attraction. However, the EDIP formalism used in these calculations does not include dispersion forces, and hence the outer radius effect is driven entirely by strain minimization. It has been suggested previously [Error! Bookmark not defined.] that space confinement is the key factor in this process, with the outer tube acting as a reaction container and templating the fused product into its final form. We confirm this hypothesis, noting the success of the present simulation due to the long times and the use of outer tubes of different radii.

The observation of templating with respect to the outer wall is reminiscent of previous EDIP simulations in which carbon sp^2 self-assembly was observed at free surfaces [16]. In those studies a thermodynamically driven process was observed in which highly ordered structures emerged from disordered precursors. By varying the geometry (i.e. the number of periodic boundary conditions) and the density of the precursor, a wide variety of ordered sp^2 structures were produced: carbon onions arose from clusters, carbon nanotubes arose from infinite wires, graphitic layers from slabs and glassy/foamy carbons from bulk material. The presence of free surfaces, be they external (due to geometry) or internal (associated with voids), was the critical physical concept connecting the different structures. These free surfaces in turn drove a templating process in which order in one region would create additional surfaces and order nearby. It is this self-assembly process which is revisited in the

present peapod simulations, with the templating effect of the outer wall representing a generalisation of the earlier EDIP work.

4. Conclusions

Using the EDIP potential for carbon, we have shown that transformation between peapods and DWCNTs can be described on the MD timescale. The calculations did not require defects to stimulate the reaction, the transformed inner tubes had a high degree of order and the correct filling factor was observed. By considering six different temperatures we show two clear regimes below the melting point of the material: (i) a polymerization step (in the 1500-2500 K range) during which the fullerenes bond with each other, and (ii) a self-assembly step (around 3500 K) in which the merged fullerene units transform into a tube. The temperature for self-assembly is virtually identical to that observed in previous EDIP simulations in which amorphous carbon is transformed into highly ordered sp^2 phases. We also demonstrate that the outer tube acts as a container for the self-assembly process, defining the inner radius as observed experimentally. This process is strain-driven with the outer tube templating the atomic rearrangements associated with the difference in radius between the initial fullerenes and the final transformed tube. The simulations also provide a physical perspective which is broader in scope than atomic-scale concepts such as Van der Waals attraction and Stone-Wales rotations. Peapod to DWCNT conversion can therefore be considered as an example of a more general phenomena, in which sp^2 carbon systems optimize their local configuration by evolving to thermodynamically favoured states in which extended surfaces are maximized and curvature is minimized.

Acknowledgements

We thank Christopher Ewels for the suggestion to explore this system and for useful discussions. Financial support from the Australian Research Council under the grant DP0986713 is gratefully acknowledged.

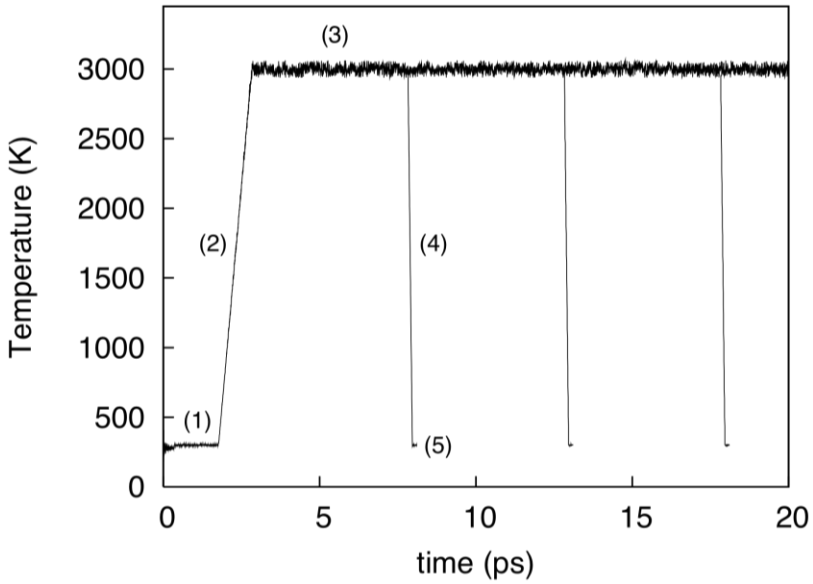

Figur

e 1. Initial stages of the annealing protocol used to induce coalescence and nanotube formation in peapods. Stage 1) Initial structure is equilibrated at 300 K prior to annealing. Stage 2) System temperature is increased to the selected anneal temperature (here 3000 K). Stage 3) System maintained at the prescribed anneal temperature and allowed to evolve for 5 ps. Stage 4) For analysis purposes, a branch simulation is initiated in which the system is cooled to 300 K. Stage 5) Thermal averages are collected at 300 K. Stages 3-5 are repeated 200 times, giving a total annealing time of 1 ns.

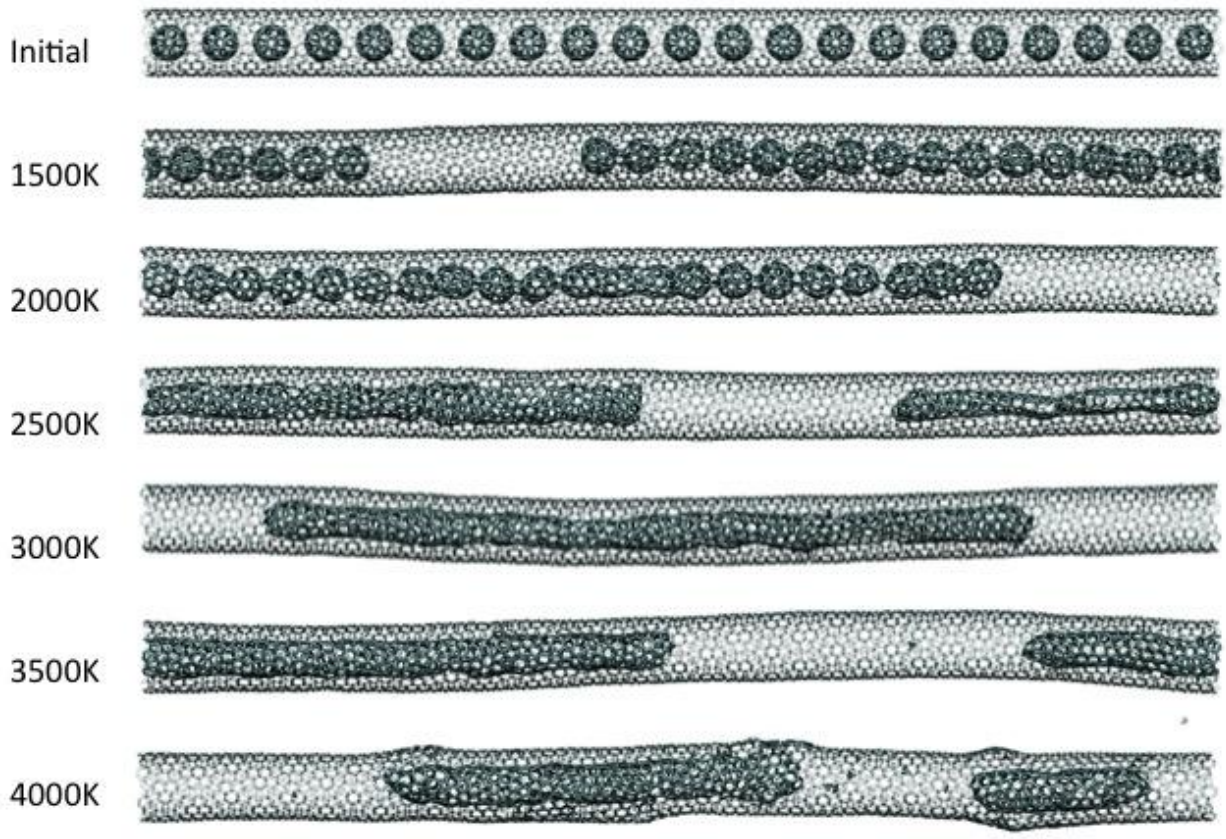

Figure 2. Snapshots of the smaller radius simulation, C_{60}@(13,7), after 1 ns of annealing at the indicated temperatures. The initial structure contains 21 equally spaced fullerenes. Coalescence is evident at 1500 and 2000 K, with DWCNT structures present at 3000 and 3500 K. At 4000 K, mass transfer between the inner and outer tubes occurs, modifying the structure and radius of the outer tube.

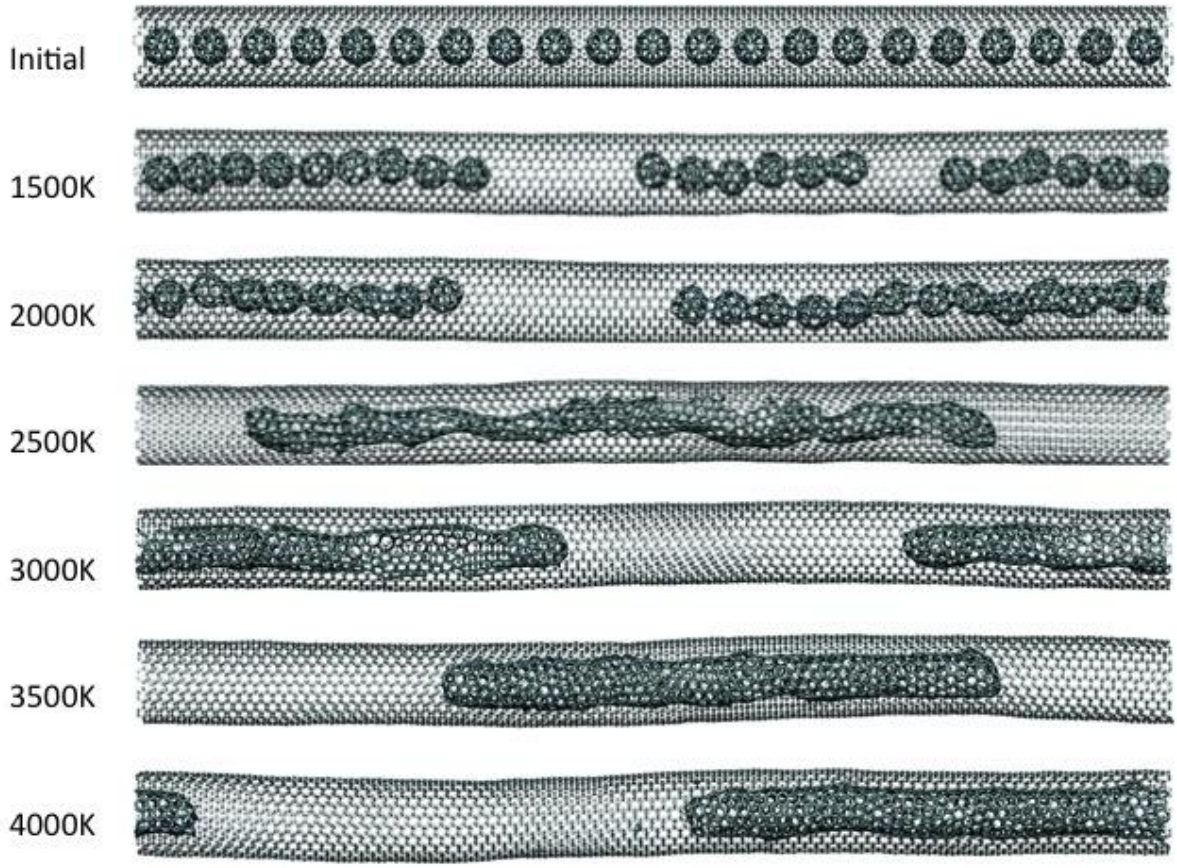

Figure 3. Snapshots of the larger radius simulation, C_{60}@(12,12), after 1 ns of annealing at the indicated temperatures. As in Figure 2, the initial structure contains 21 equally spaced fullerenes, and the supercell length is the same. Coalescence at low temperatures is less ordered due to the large internal volume. Due to reduced strain effects, formation of DWCNT occurs over a broader temperature range, and mass transfer is not seen at 4000 K.

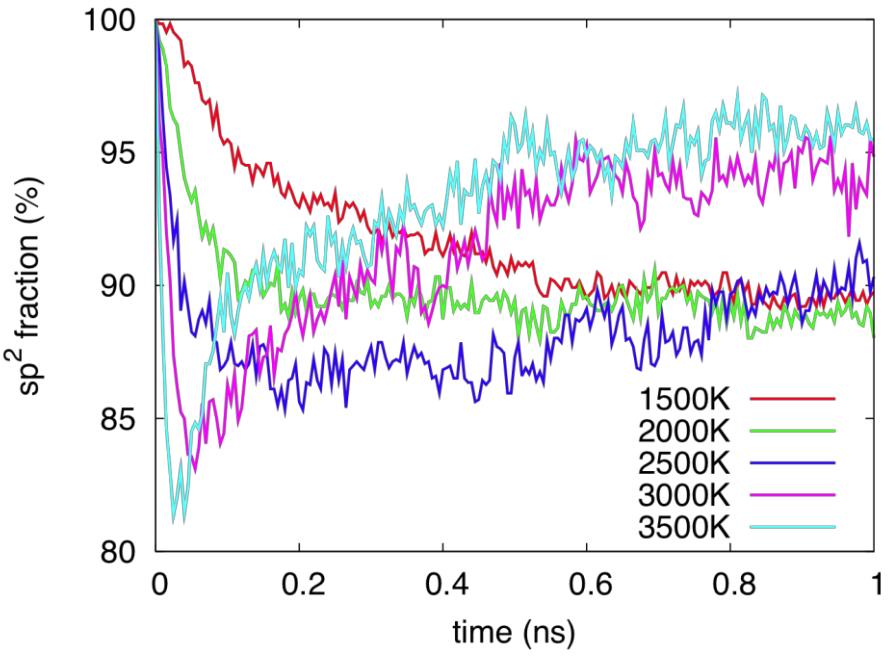

Figure 4. Percentage of sp^2 bonded atoms (three-fold coordinated, 1.85Å cutoff) as a function of time and temperature for the C60@(13,7) system. All analysis is performed at 300 K (stage 5 in Figure 1) and only the 1260 atoms initially present in the fullerenes are considered.

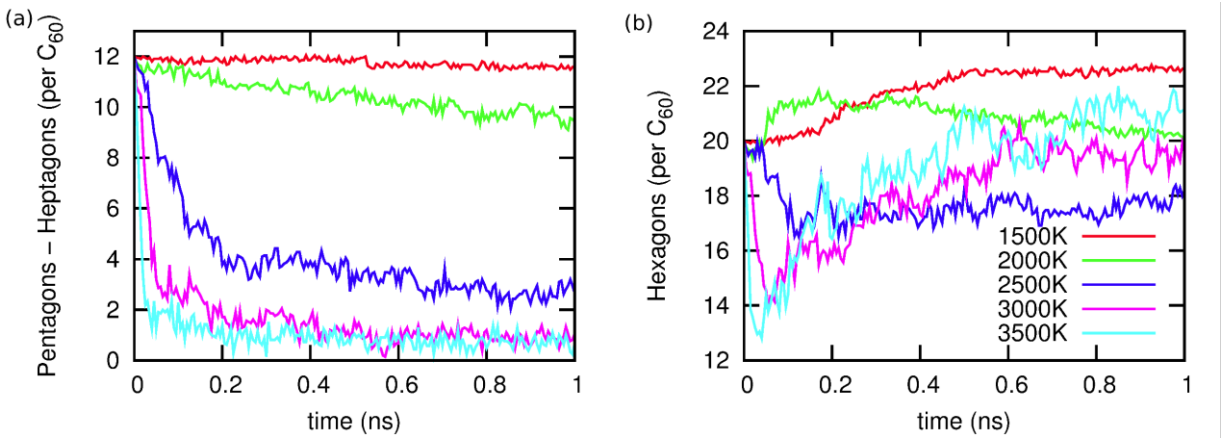

Figure 5. Ring statistics as a function of time and temperature for the C_{60}@(13,7) system. All analysis is performed at 300 K (stage 5 in Figure 1) and only the 1260 atoms initially present in the fullerenes are considered.

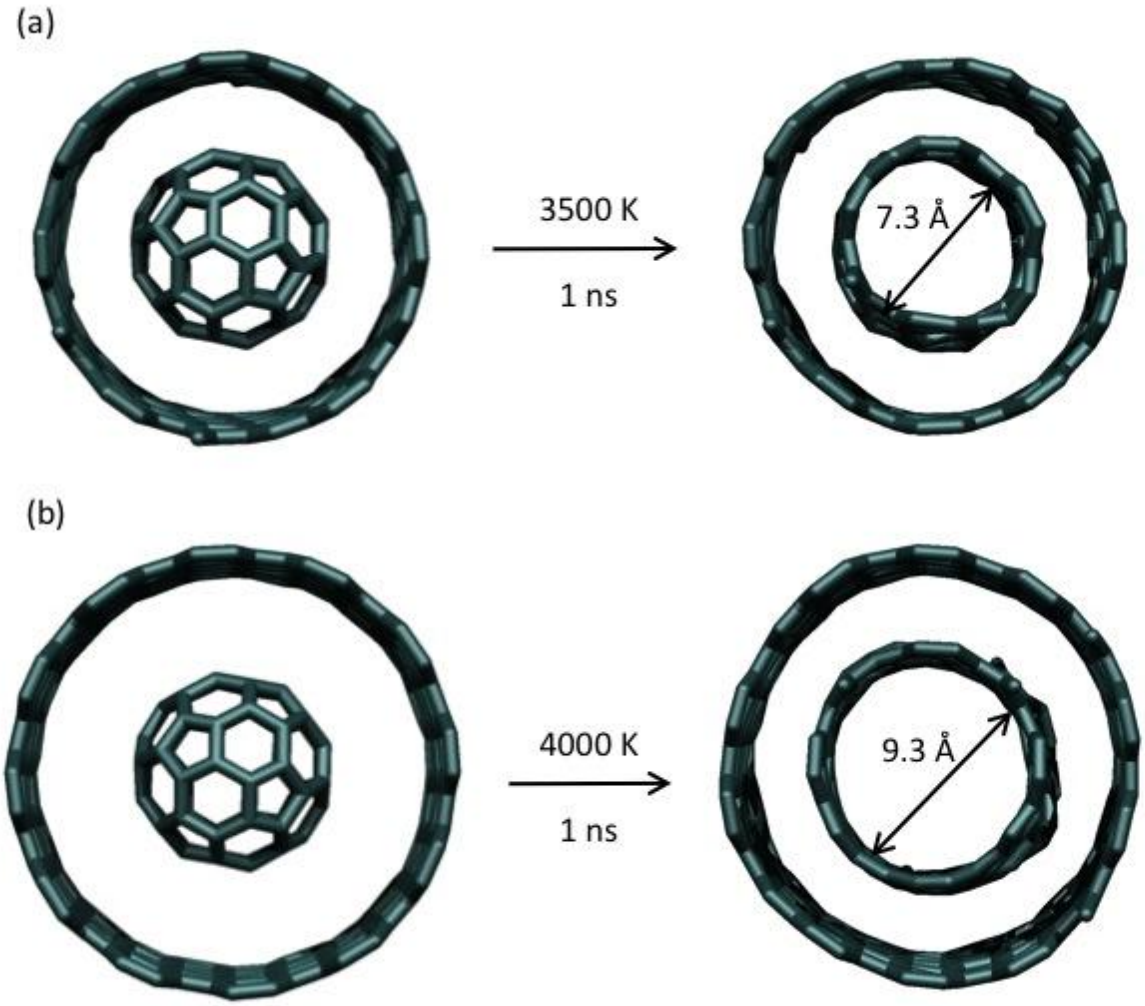

Figure 6. Views along the tube axis of the (a) (13,7) and (b) (12,12) systems. Left: Initial structures; Right: final structures after annealing under the conditions shown. The diameter of the transformed (inner) nanotube is denoted by the arrows. Note that the inner tube diameter is strongly dependent on the diameter of the outer tube.

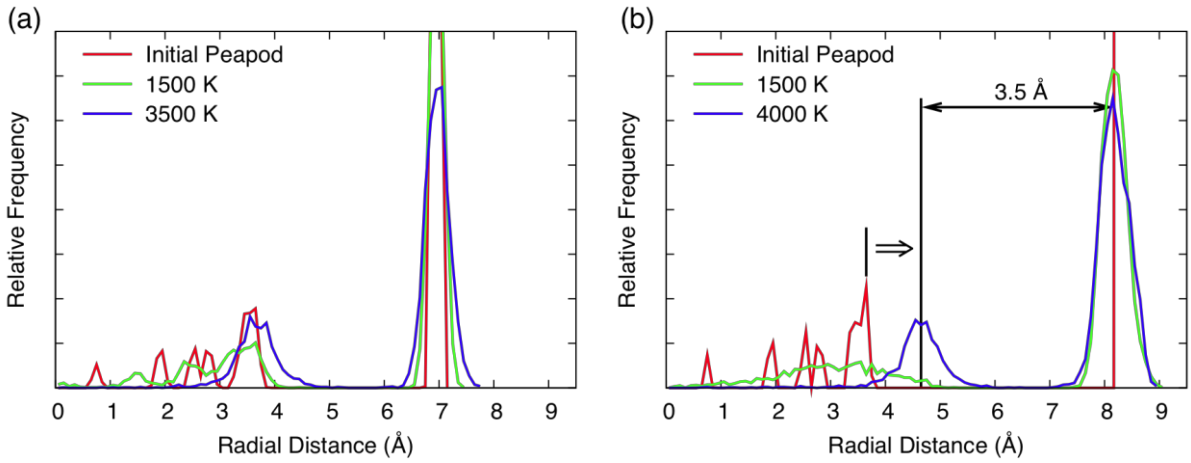

Figure 7. Radial distribution profiles with respect to the tube axis for the a) (13,7), and b) (12,12) systems. As described in the text, the centre of mass is used to define the tube axis in each 1 nm slab. For the (12,12) system there is a radial expansion of the inner tube indicated by the white arrow. This reduces the inter-tube spacing to 3.5 Å as indicated on the graph.

References

[1] Smith BW, Monthioux M, Luzzi DE. Encapsulated C60 in carbon nanotubes. Nature 1998;396:323-324

[2] Luzzi DE, Smith BW. Carbon cage structures in single wall carbon nanotubes: a new class of materials. Carbon 2000;38:1751–6

[3] Kataura H, Maniwa Y, Kodama T, Kikuchi K, Hirahara K, et al. High-yied fullerene encapsulaption in single-wall carbon nanotubes. Synthetic Metals 2001;121:1195-1196

[4] Chorro M, Delhey A, Noe L, Monthioux M, Launois P. Orientation of C-70 molecules in peapods as a function of the nanotube diameter. Phys Rev B 2007;75(3):03416—1-11

[5] Eliasen A, Paaske J, Flensberg K, Smerat S, Leijnse M, Wegewijs M.R, et al. Transport via coupled states in a C60 peapod quantum dot. Phys. Rev. B. 2010;81:155431—1-5

[6] Pichler T, Kukovecz A, Kuzmany H, Kataura H, Achiba Y. Quasicontinuous electron and hole doping of C60 peapods. Phys. Rev. B 2003;67:125416—1-7

[7] Kataura H, Maniwa Y, Abe M, Fujiwara A, Kodama T, et al. Optical properties of fullerene and non-fullerene peapods Appl. Phys. A 2002;74:349–354

[8] Bandow S, Takizawa M, Hirahara K, Yudasaka M, Iijima S. Raman scattering study of double-wall carbon nanotubes derived from the chains of fullerenes in single-wall carbon nanotubes. Chem Phys Lett 2001;337(1-3):48-54

[9] Luzzi DE, Smith BW. Carbon cage structures in single wall carbon nanotubes: a new class of materials. Carbon 2000;38(11-12):1751-1756

[10] Hernández E, Meunier V, Smith BW, Rurali Rm Terrones H Buongioro Nardelli M et al. Fullerene coalescence in nanopeapods: A path to novel tubular carbon. Nano Lett 2003;3(8):1037-1042

[11] Hodak M, Girifalco LA. Ordered phases of fullerene molecules formed inside carbon nanotubes. Phys Rev B 2003; 67:075419—1-4

[12] Zhao Y, Yakobson B, Smalley R. Dynamic Topology of Fullerene Coalescence. Phys Rev Lett 2002;88(18):185501—1-4

[13] Han S, Yoon M, Berber S, Park N, Osawa E, Ihm J et al. Microscopic mechamisn of fullerene fusion. Phys Rev B 2004;70:113402—1-4

[14] Launois P, Chorro M, Verberck B, Albouy P-A, Rouziére S, Colson D et al. Transformation of C70 peapods into double walled carbon nanotubes. Carbon 2010;48:89-98

[15] Su H, Nielsen RJ, van Duin ACT, Goddard III WA. Simulations on the effects of confinement and Ni-catalysis on the formation of tubular fullerene structures from peapod precursors. Phys Rev B 2007;75:134107—1-5

[16] Powles RC, Marks NA, Lau DWM. Self-assembly of sp(2)-bonded carbon nanostructures from amorphous precursors. Phys Rev B 2009;79(7): 075430—1-11

[17] Marks NA. Generalizing the environment-dependent interaction potential for carbon. Phys Rev B 2001;63(3):035401—1-7

[18] Marks N. Modellind diamond-like carbon with the environment-dependent interaction potential. J. Phys.: Condens. Matter 2002;14:2901–2927

[19] Lau DWM, McCulloch DG, Marks NA, Madsen NR, Rode AV. High-temperature formation of concentric fullerene-like structures within foam-like carbon:

Experiment and molecular dynamics simulation. Phys Rev B 2007;75(23):233408—1-4

[20] Justo JF, Bazant MZ, Kaxiras SE, Bulatov VV, Yip S. Interatomic potential for silicon defects and disordered phases. Phys Rev B 1998;58(5):2539-2550

[21] Nordlund K, Keinonen J and Mattila T. Formation of Ion Irradiation Induced Small-Scale Defects on Graphite Surfaces. Phys Rev Lett 1996;77(4):699-702

[22] Kaukonen HP and Nieminen RM. Molecular-Dynamics simulation of the growth of diamond-like films by energetic carbon-atom beams. Phys Rev Lett 1992;68(5):620-623

[23] Stephan U and Maase M. A molecular-dynamics study and the electronic-properties of amorphous-carbon using the Tersoff potential. J Phys Condens Matter 1993;5:9157-9168

[24] Jäger HU and Albe K. Molecular-dynamics simulations of steady-state growth of ion-deposited tetrahedral amorphous carbon films. J Appl Phys 2000;88(2):1129-1135

[25] Marks NA, Cooper NC, McKenzie DR, McCulloch DG, Bath P, Russo SP. Comparison of density-functional, tight-binding, and empirical methods for the simulation of amorphous carbon. Phys Rev B 2002;65(7):075411—1-9

[26] Kroto HW, Heath JR, O'Brien SC, Curl RF, Smalley RE. C-60 – Buckminsterfullerene. Nature 1985;318(6042):162-163

[27] Patchovskii S and Thiel W. C60 Dimers: A Route to Endohedral Fullerene Compounds?. J Am Chem Soc 1998;120:556-563

[28] Matsuzawa N, Ata M, Dixon DA, Fitzerald G. Dimerization of C60: The Formation of Dumbbell-Shaped C120. J Phys Chem 1994;98:2555-2563

[29] Terrones H, Terrones M, Hernandez E, Grobert N, Charlier JC, Ajayan PM. New metallic allotropes of planar and tubular carbon. Phys Rev Lett 2000;84(8):1716-1719

Figure 1

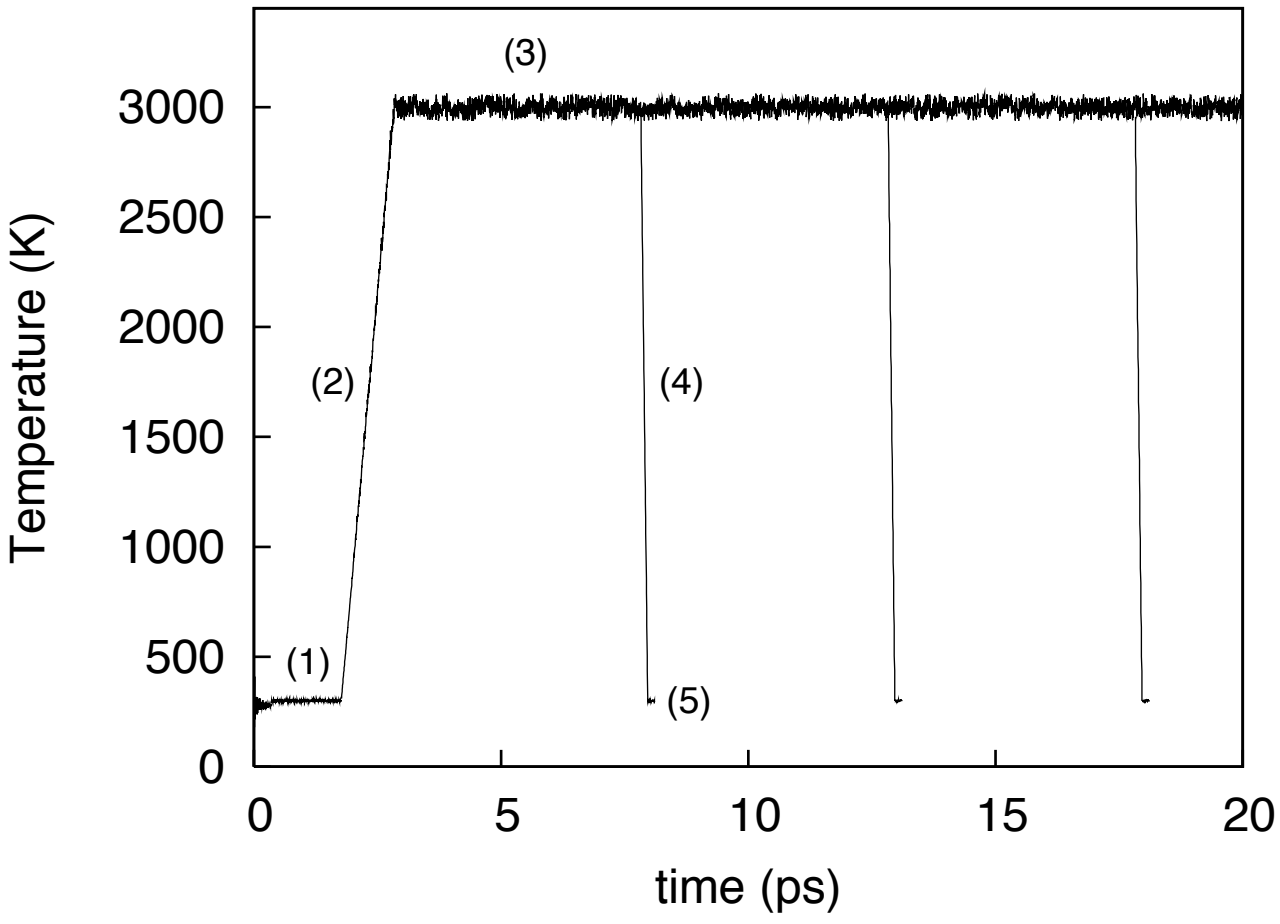
Temperature (K)
3000
2500
2000
1500
1000
500
0
0
5
10
15
20
time (ps)
(1)
(2)
(3)
(4)
(5)

Figure 2

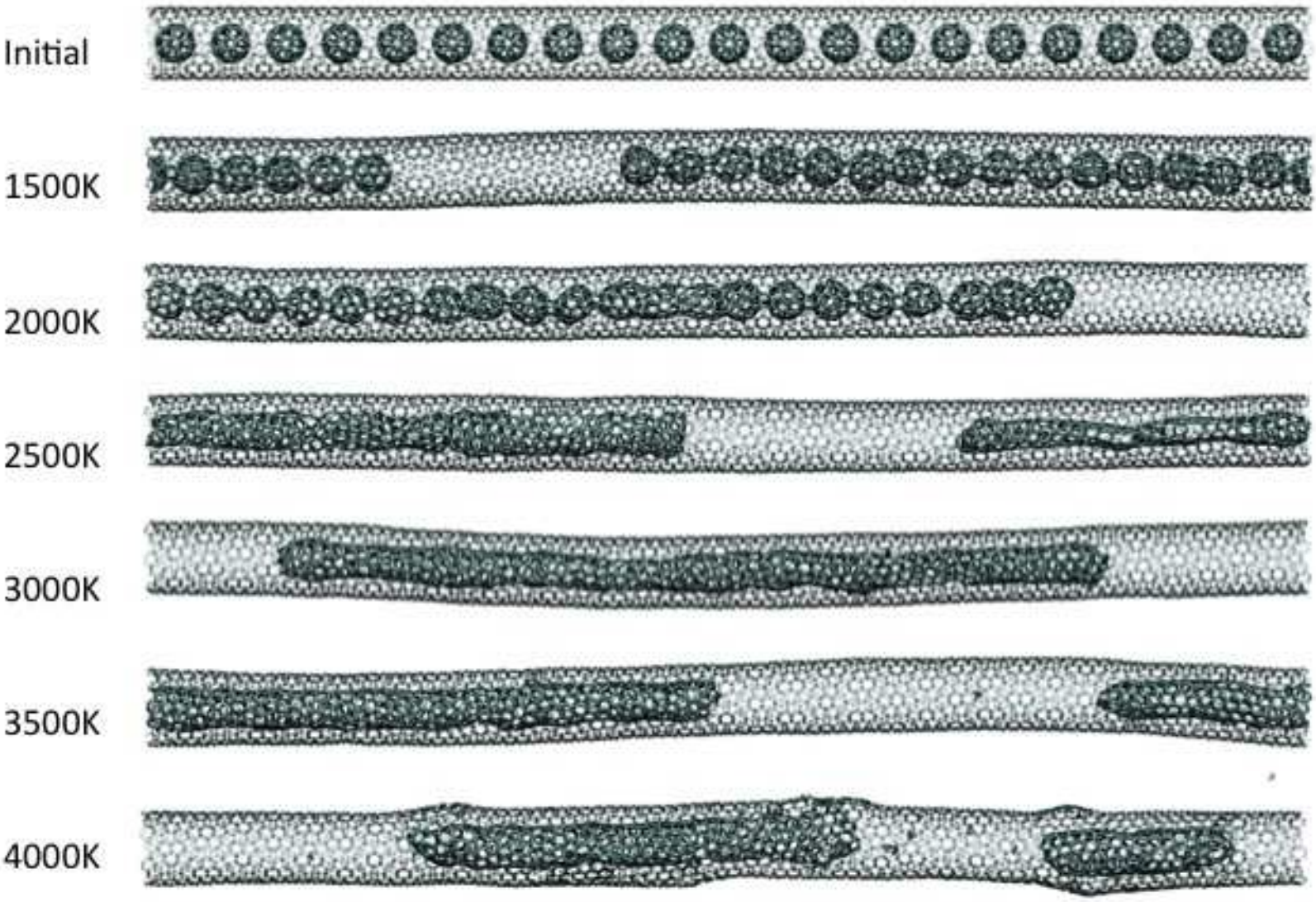

Figure 3

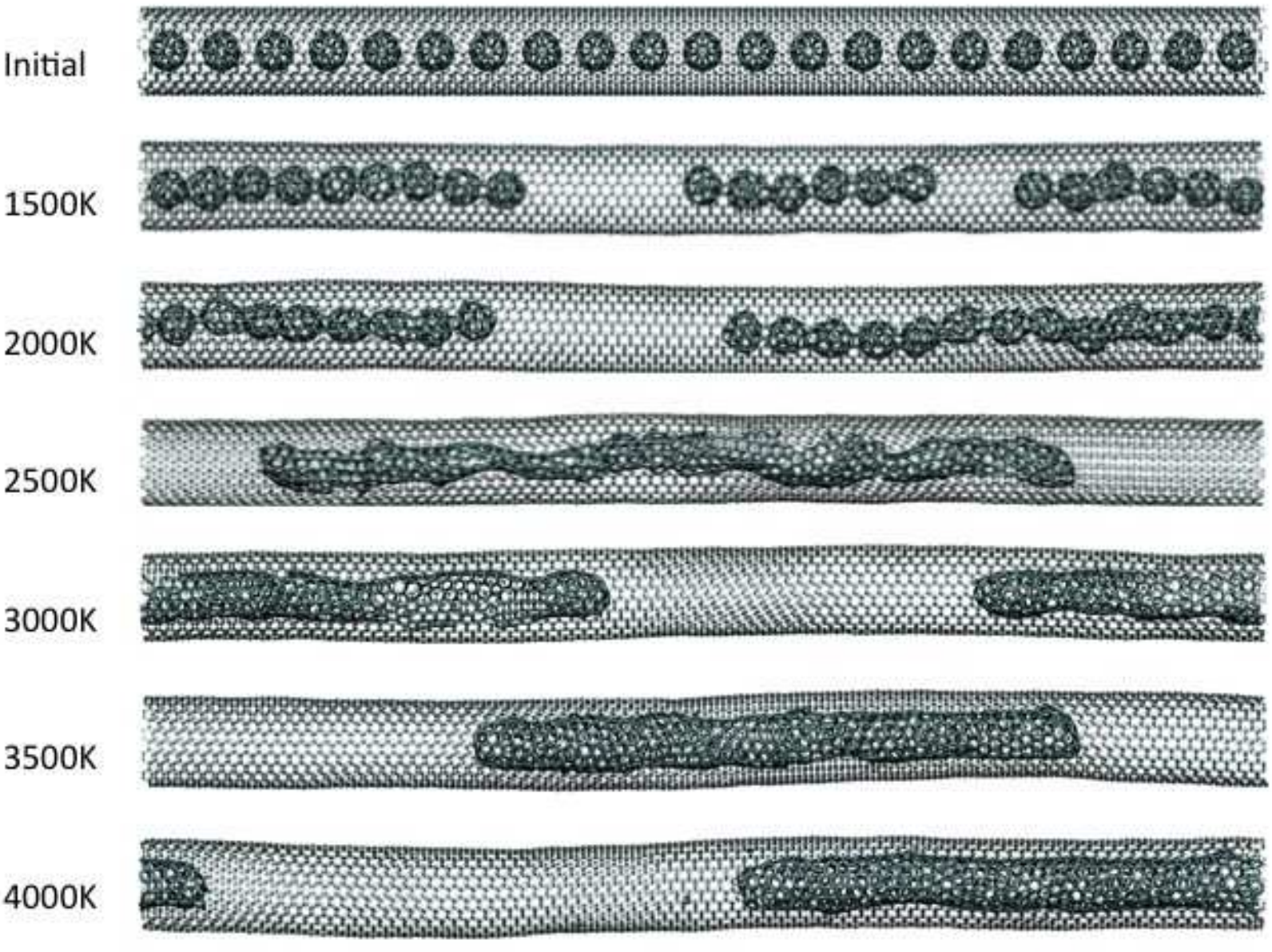

Figure 4

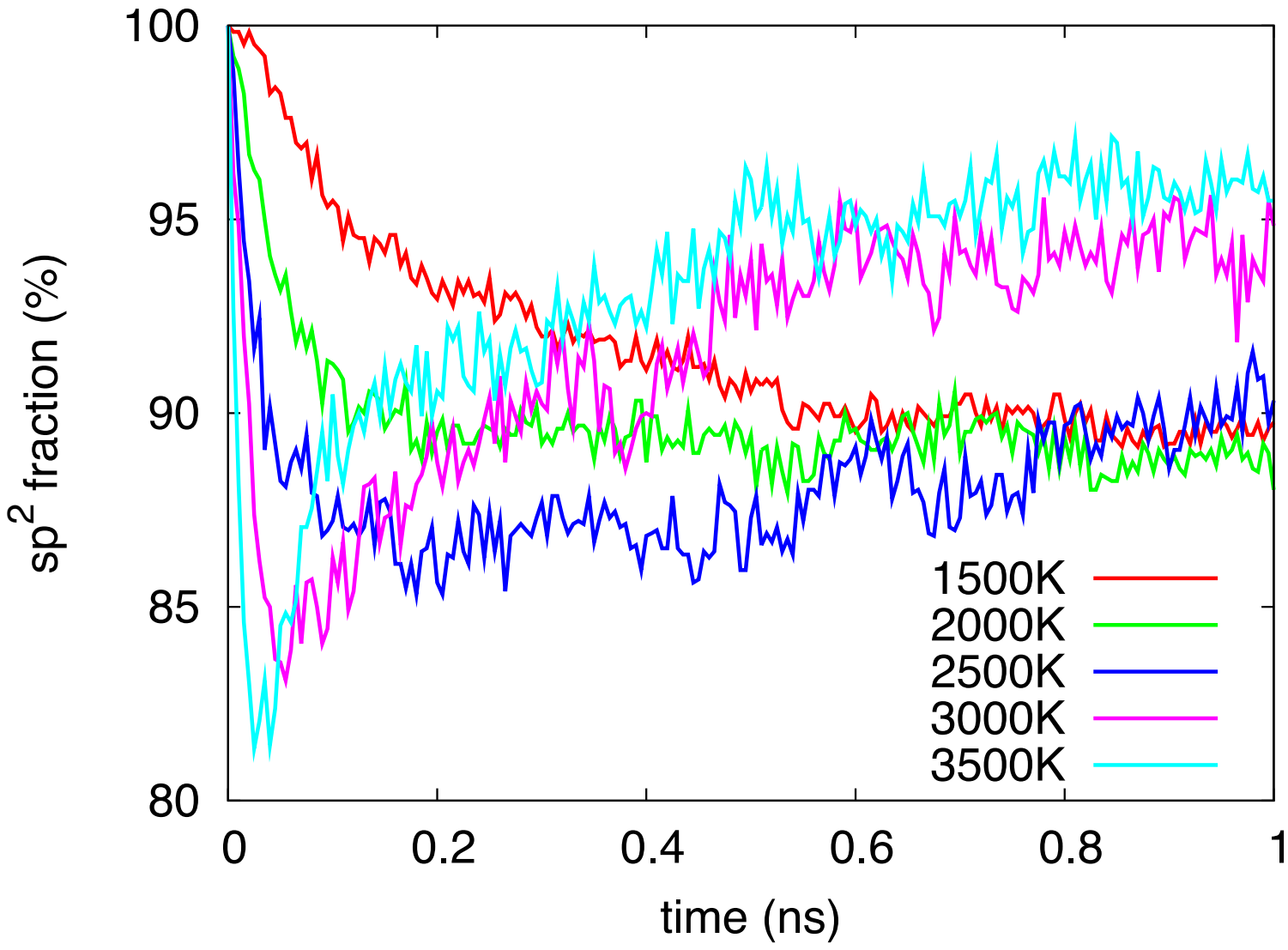
100
95
90
85
80
0
0.2
0.4
0.6
0.8
1
sp2 fraction (%)
time (ns)
1500K
2000K
2500K
3000K
3500K

Figure 5

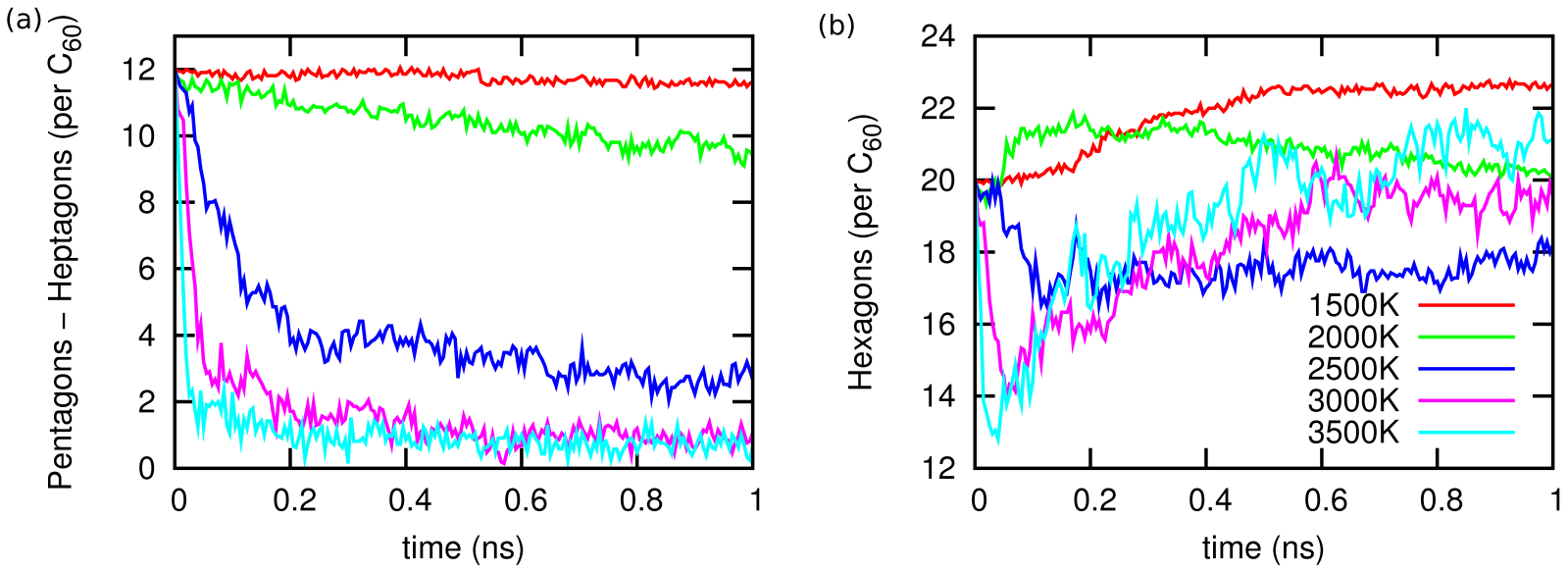
(a)
Pentagons – Heptagons (per C_{60})
time (ns)
(b)
Hexagons (per C_{60})
time (ns)
1500K
2000K
2500K
3000K
3500K

Figure 6

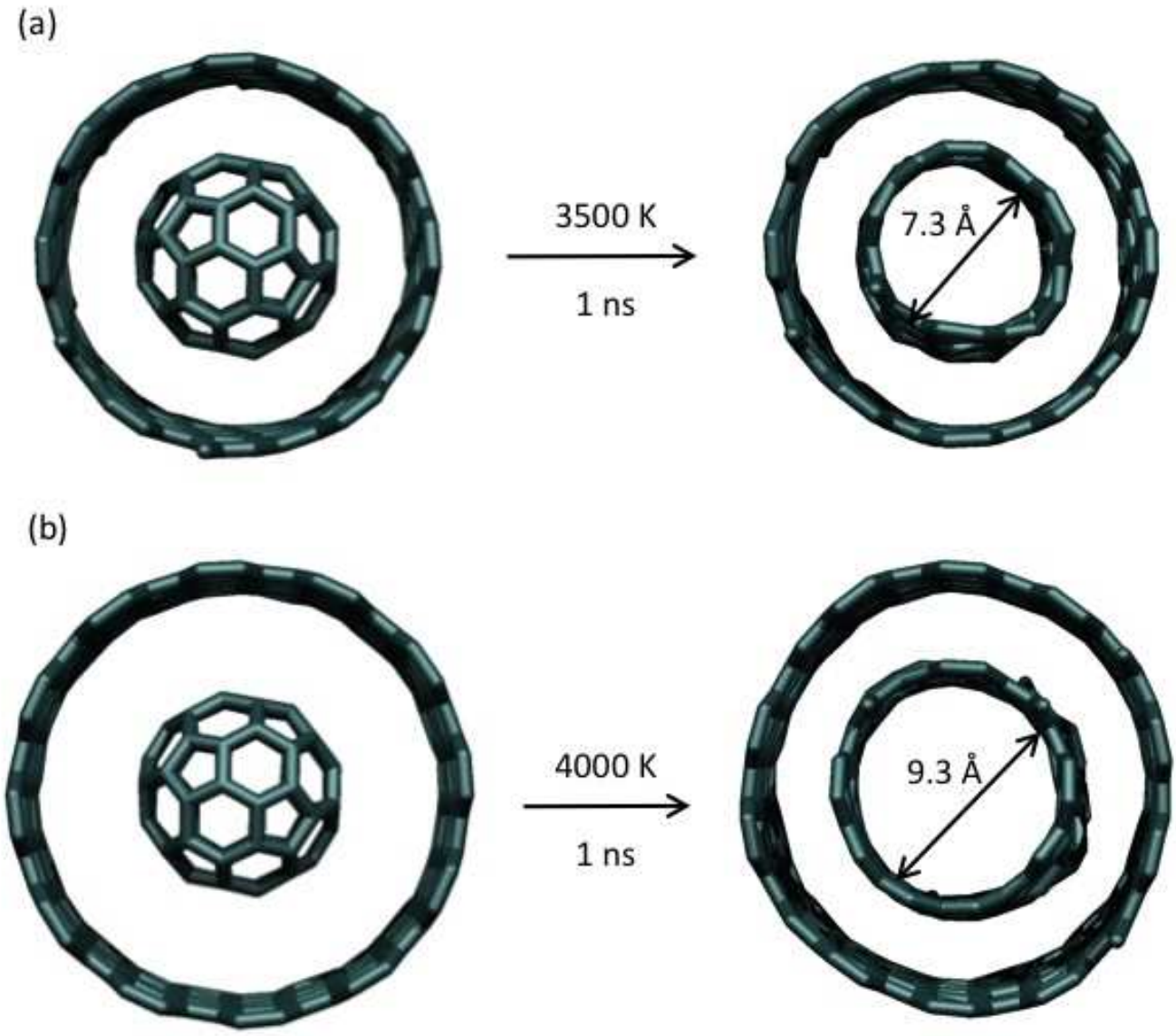

Figure 7

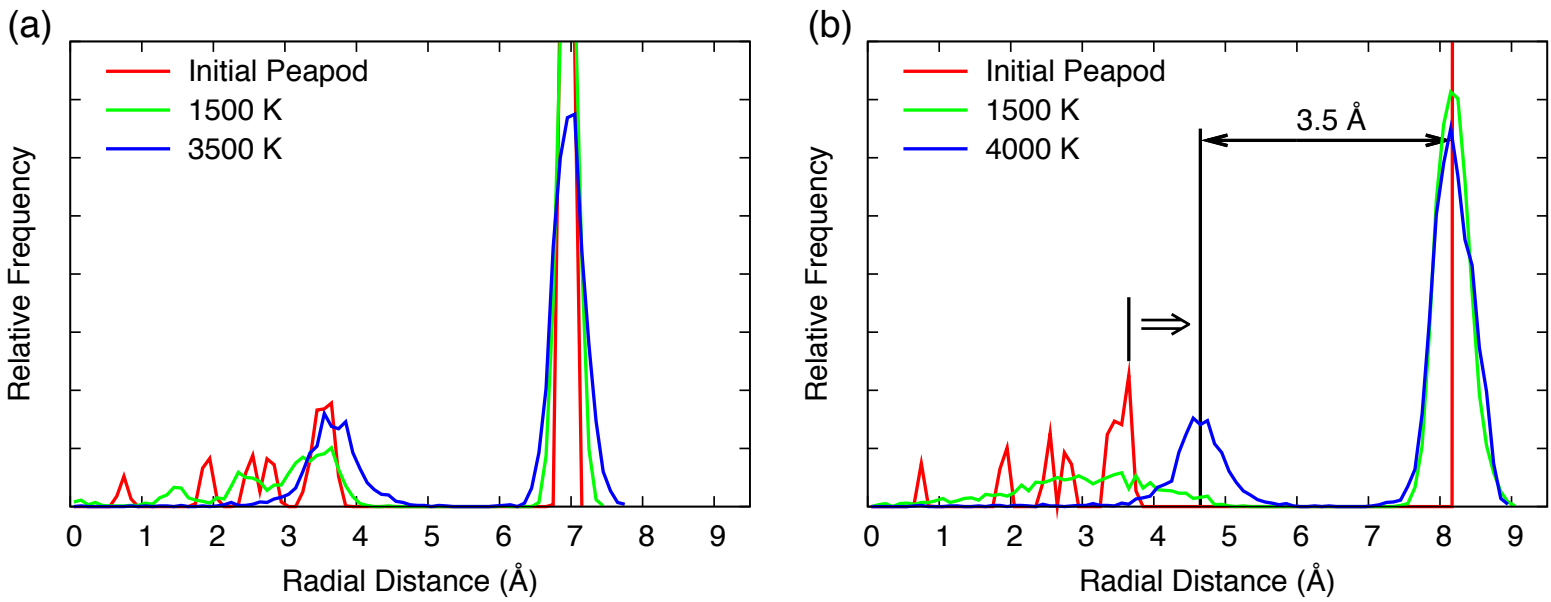
(a)
Initial Peapod
1500 K
3500 K
Relative Frequency
0
1
2
3
4
5
6
7
8
9
Radial Distance (Å)
(b)
Initial Peapod
1500 K
4000 K
3.5 Å
Relative Frequency
0
1
2
3
4
5
6
7
8
9
Radial Distance (Å)